Oil Shale, 2015, Vol. 32, No. 2, pp. 134–150
doi: 10.3176/oil.2015.2.04
ISSN 0208-189X

CHARACTERIZATION OF DACHENGZI OIL SHALE FAST PYROLYSIS BY CURIE-POINT PYROLYSIS-GC-MS

YIRU HUANG, XIANGXIN HAN, XIUMIN JIANG*

Institute of Thermal Energy Engineering, School of Mechanical Engineering, Shanghai Jiao Tong University, Shanghai, 200240, PR China

Abstract. *Fast pyrolysis of a Dachengzi oil shale sample was studied using a Curie-point pyrolyzer, the pyrolysis products were characterized online by gas chromatography-mass spectroscopy. Nine different Curie-point temperatures were chosen to investigate product distribution regularities. Hydrocarbons were the major components of the fast pyrolysis products of oil shale. n-Alkanes were generated at all the nine temperatures, while cycloalkanes only appeared at the temperatures above 485 °C. Branched alkanes were seldom produced at all the temperature points because of the bond cleavage at the branch point. Alkenes and aromatic compounds began to be formed at 386 °C and 423 °C separately, and their molecule sizes decreased with increasing pyrolysis temperature. Various oxygen-containing compounds, including ketones, acids, alcohols, esters and phenols, were identified in the shale oil components, indicating the wide existence of oxygen-containing functional groups.*

Keywords: *oil shale, pyrolysis, GC-MS, Curie-point, fast pyrolysis.*

1. Introduction

Oil shale is defined as a fine-grained sedimentary rock which can produce oil through pyrolysis in the absence of air [1]. With the second largest reserve in solid fossil fuels, it is deemed as one of the most promising sources of substitutes for petroleum [2]. The pyrolysis products of oil shale include oil, gas and char [3, 4]. The amount and quality of the shale oil produced are the most focused aspects which will determine the process feasibility both technically and economically [1]. Compared with conventional crude oil, shale oil has higher contents of heteroatomic compounds which will cause troubles during utilization such as fuel instability and air

* Corresponding author: e-mail *xiuminjiang@sjtu.edu.cn*

pollution [5, 6]. Consequently, it is important to identify the chemical composition of shale oil and study its variation trends under different conditions.

Many researches have been done on the shale oil properties. Rovere et al. [7] separated the chemical classes of shale oils by low pressure liquid chromatography. Fletcher et al. [8] identified the carbon types in shale oil by ^{13}C NMR and studied their relations with pyrolysis conditions. Tong et al. [9] studied the characteristics of nitrogen-containing species in Huadian shale oil by electrospray ionization Fourier transform ion cyclotron resonance mass spectrometry and found that the basic nitrogen classes in Huadian shale oil include N_1, N_1O_1, N_1O_2, N_1O_3, N_1S_1 and N_2 classes. Tiwari et al. [1] made the compositional analysis of oil shale using TGA-MS to study the changes in the products distribution during the pyrolysis process.

Among all the analysis methods, pyrolysis coupled with gas chromatographic separation and mass spectroscopic detection (Py-GC-MS) plays a very important role in the field of analytical pyrolysis. The gas chromatography-mass spectroscopy (GC-MS) analysis is a widely used method to evaluate the oil products of pyrolysis in both fossil and biomass fuels [10–12]. The shale oil compositional measurements have been taken using GC-MS in many studies [13–15]. Py-GC-MS allows direct chromatographic separation of the gaseous products evolved from the pyrolysis process. It has been reportedly used in the identification of pyrolysis products of biomasses and fossil fuels [16–19].

Heating rate is one of the most important parameters which affect the pyrolysis process, including the release and composition of volatiles [20]. Based on heating rate, the process is generally divided into four types: slow, medium, fast and flash. The respective heating rates are of the order of magnitude of 10^1 K/s, 10^2–10^3 K/s, 10^4–10^5 K/s and up to 10^6 K/s [21]. Niksa and Lau [22] did researches on various coal types and found that when the heating rate increased by one order of magnitude, the pyrolysis rate would increase five times. Yanik et al. [23] investigated both slow and fast pyrolysis of oil shale samples from the Göynük Himmetoğlu deposit, and noticed that the oil yield by fast pyrolysis (35.1% at 550 °C) was much higher than that in slow pyrolysis (23.0% at 550 °C). The fast pyrolysis extract had a much higher proportion in the aliphatic fraction with a chain length longer than C_{20}. The secondary cracking reactions of products occurring during the slow pyrolysis raised the uncondensable gas yield and at the same time made the oil yield, especially heavy oil yield, decrease. On the contrary, secondary cracking reactions in the fast pyrolysis were reduced to a large extent, leading to the higher oil yield and heavy fraction proportion. It is necessary to conduct researches on fast pyrolysis systematically to get knowledge about the pyrolysis process and reaction mechanisms.

A Curie-point pyrolyzer is a high-frequency induction heating pyrolysis instrument of medium heating rate. The heating rate of the Curie-point pyrolyzer may reach 5000 °C/s, which means that it only needs 0.1–0.2 s to heat the sample from room temperature to the reaction temperature.

Consequently, the sample undergoes homogeneous thermal decomposition at a specific temperature. The Curie-point pyrolyzer combined with a gas chromatographic separator and a mass spectroscopic detector (CP-GC-MS) may give accurate qualitative and quantitative analytical data on the organic substances in the pyrolysis products without pre-treatment or separation. CP-GC-MS is a widely used apparatus in pyrolysis analysis of biomass, coal, oil shale, etc. [24–27], and offers excellent accuracy, sensitivity, specificity and reproducibility [28]. In this article, the CP-GC-MS method is used to study the distribution of the pyrolysis products of Dachengzi oil shale at nine different temperatures and thus get knowledge about the fast pyrolysis regularities and information on the kerogen macromolecular structure.

2. Experimental section

2.1. Oil shale sample preparation

The oil shale sample analyzed in this work was obtained from Dachengzi mine located in Huadian city, China. Results of proximate and ultimate analyses of the sample are given in Table 1. Considering the National Standards of China (GB 474-1996), the oil shale sample was sampled, crushed, ground, and sieved to the size range of 0–0.25 mm, and then stored in a desiccator for use.

Table 1. Proximate and ultimate analyses of the oil shale sample, wt%, ar [a]

Proximate analysis					Ultimate analysis				
M	V	A	FC	Q_{net}, MJ/kg	C	H	O	N	S
11.54	36.20	48.24	4.02	11.08	27.33	3.59	7.89	0.57	0.84

ar – on an as-received basis; [a] – O content was calculated by difference.

2.2. Instruments and methods

The fast pyrolysis experiments of Dachengzi oil shale were conducted on a set of combined instruments including a Curie-point pyrolyzer, a gas chromatograph and a mass spectrometer. The whole experiment process could be classified into two main parts – pyrolysis and analysis. The pyrolysis process took place in a JHP-5 Curie-point pyrolyzer, while the analysis process was carried out with an Agilent 6890N/5973N gas chromatograph-mass spectrometer. The gas outlet of the pyrolyzer was connected to the sample introduction chamber of the GC-MS by a connecting tube heated to 350 °C. The schematic diagram of the CP-GC-MS system has been shown in [29].

In the Curie-point pyrolyzer, the pyrolysis temperature was dependent on the material properties of the ferromagnetic foils in which the sample was wrapped. Foils made with different ferromagnetic materials had different Curie-point temperatures. The ferromagnetic foils were induction heated by

a radio frequency field. Therefore, they could rapidly reach the Curie-point temperatures of ferromagnetic materials in less than 100 ms. At the Curie-point temperatures, the materials would lose their magnetic properties so that very precisely controlled temperatures were obtained. Nine independent tests using nine different ferromagnetic foils with Curie-point temperatures of 225, 280, 315, 386, 423, 485, 590, 650 and 764 °C, respectively, were conducted under He atmosphere in this research. In each test, about 1 mg sample was applied and the reaction time was 5 s. The pyrolysis products in the Curie-point pyrolyzer were transferred online to the GC-MS instruments to identify the components.

In gas chromatography, the column used was a 30 m HP-5 MS fused silica capillary column (I.D. 0.25 mm, film thickness 0.25 μm). The temperature of the GC oven was kept at 45 °C for 4 min and subsequently programmed to 280 °C at 3 K/min and then kept for 15 min. The inlet temperature was 250 °C and the detector temperature was 280 °C. Helium was adopted to be the carrier gas with a flow rate of 1.0 mL/min, and the split ratio was 100:1. The mass spectrometer was operated at 70 eV in the electron ionization mode, scanning from 50 to 550 amu. The ion source temperature was 230 °C. The pyrolysis products were identified and analyzed by searching the NIST11 mass spectrometry library, and the software of Agilent MSD Productivity ChemStation. The product contents were determined by the area normalization method. Compound concentrations were calculated by integrating their corresponding gas chromatographic peak areas and the summed areas of the peaks were normalized to 100%. To ensure the reproducibility of experiments, each test was conducted twice.

3. Results and discussion

The most dominant Dachengzi shale oil components of Curie-point pyrolysis were aliphatic hydrocarbons. This is consistent with the solid-state ^{13}C NMR results obtained by Tong et al. [30] who established that the carbon skeletal structure of this kerogen consisted of 86.1% of a fairly high aliphatic carbon fraction. This also agrees with the results of the Curie-point pyrolysis conducted with Mol, Bure and Tournemire oil shales at 358 °C and 650 °C [27].

In the CP-GC-MS tests, oil yields were hard to estimate. To estimate the oil yields at different temperatures, the total ion current peak area per milligram sample was used to give general information about the yields. Figure 1 shows the variation of the total peak area per milligram oil shale sample by contrasting with the maximum value. It can be seen that at low temperatures the cracking reaction of kerogen was not intense. However, at about 400 °C there was an obvious increase in oil yield, indicating that the pyrolysis process strengthened. There was a maximum point at about 550 °C, and then the oil yield decreased with increasing temperature.

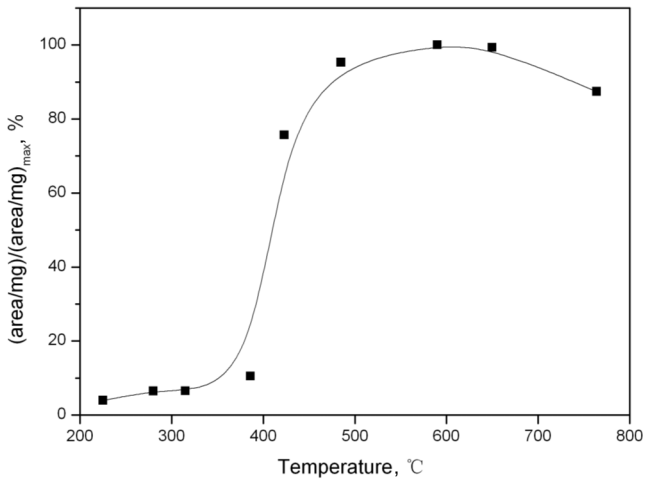

Fig. 1. Variation of total peak area per unit oil shale sample.

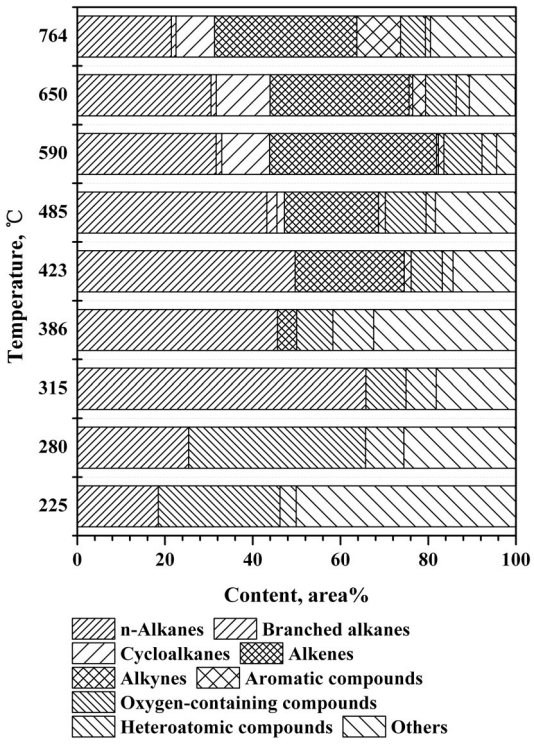

Fig. 2. Distribution of pyrolysis products at different Curie-point temperatures. ("Others" stands for the components not identified with enough match quality.)

Figure 2 shows the distribution of the main classes of components of the shale oils obtained at different Curie-point temperatures. At temperatures

below 400 °C, the pyrolysis reactions were quite slow so that only a few products were generated. At lower temperatures the clearly defined components (match quality > 80%) included mainly alkanes, oxygen-containing compounds and some heteroatomic compounds. When the temperature was higher than 400 °C, the reactions became intense, affording large amounts of alkenes, cycloalkanes and aromatic compounds in the oil components.

3.1. Distribution of alkanes

Alkanes in the oils are, according to structure, divided into three classes: n-alkanes, branched alkanes and cycloalkanes, their distribution is shown in Figure 2.

3.1.1. Distribution of n-alkanes

As noted in the literature [31, 32], aliphatic hydrocarbons are the major components of shale oil. Yürüm and Levy [32] carried out researches on the fractions of crude shale oil and found that the content of aliphatics was 53.45%. Figure 3 shows the distribution of n-alkanes at nine different Curie-point temperatures. It can be seen that as the temperature increased, the alkane species amount increased obviously, indicating that the decomposition reaction was intensified with the change of temperature. At 225 and

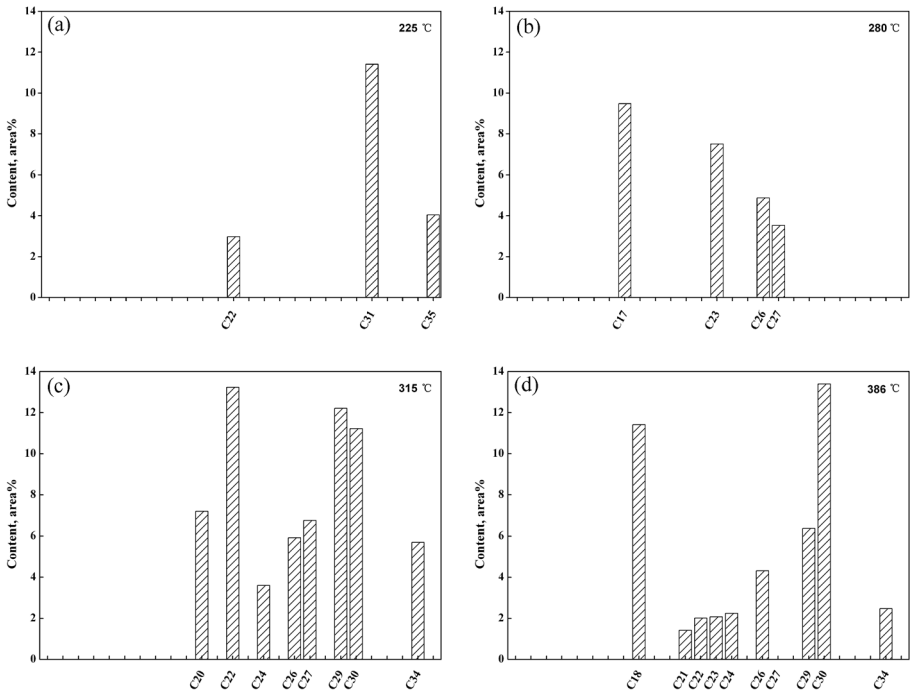

Fig. 3. Distribution of n-alkanes at different Curie-point temperatures.

Fig. 3 (Continuation)

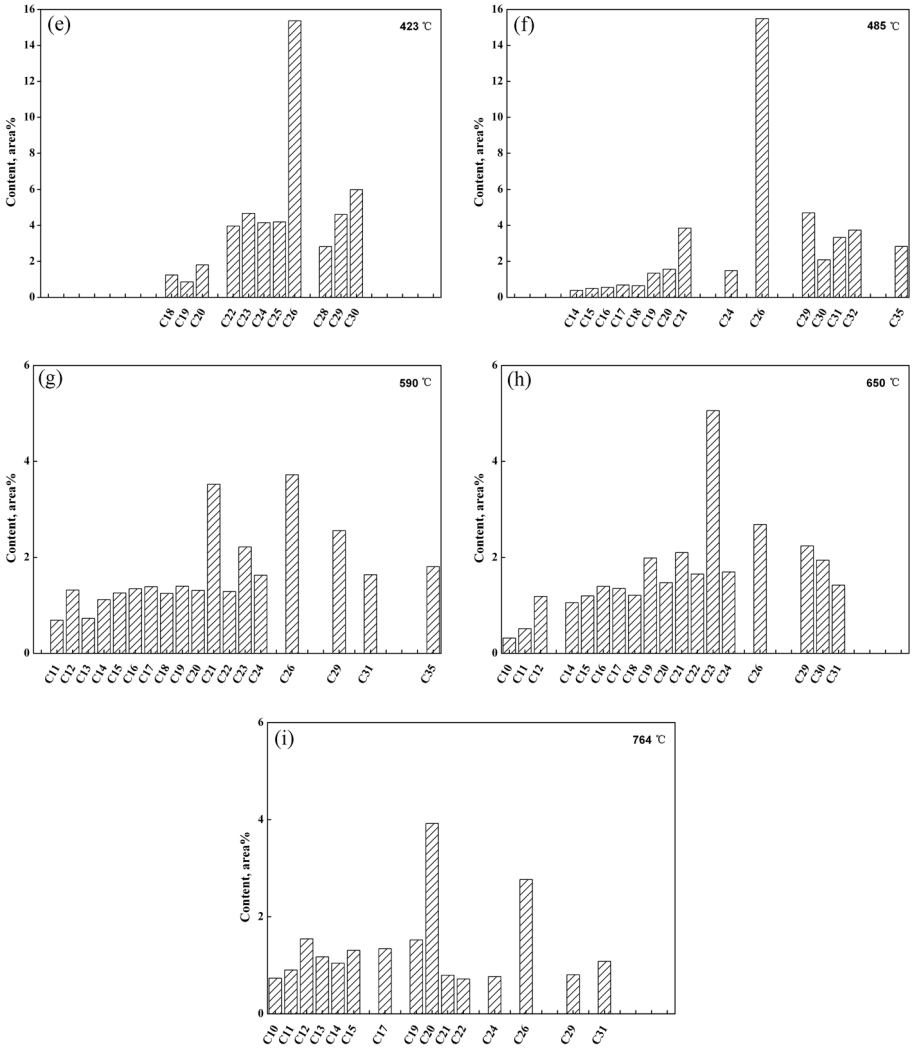

280 °C, there were only few alkanes in the components. When the temperature was below or equal to 423 °C, n-alkanes with a carbon number smaller than 20 seldom appeared, but when the temperature was above 423 °C, their amount increased gradually with increasing temperature. At higher temperatures, alkanes were partly generated from the cracking of kerogen, while the other part resulted to some extent from the thermal cracking of hydrocarbons. The long-chain alkanes got cracked via a free radical reaction mechanism, producing an olefin and a shorter alkyl radica1 [33]. Then the new radical would either crack further or form a new short-chain alkane by combination with a hydrogen radical [34].

3.1.2. Distribution of branched alkanes

Advanced analysis of alkanes revealed that branched alkanes rarely appeared in the pyrolysis products. When the temperature was below 485 °C, there were no branched alkanes in the oils generated; when the temperature was equal to or above 485 °C, only one or two kinds of branched alkanes were identified in the oils. 2,6,10,14-Tetramethyl-7-(3-methylpent-4-enylidene) pentadecane was identified in the pyrolysis products when the temperature was equal to or above 590 °C, indicating that this compound is a part of the kerogen macromolecular structure. The rare existence of branched alkanes proves that the C–C bond at the branched point of the kerogen macromolecular structure is much easier to break, so that n-alkanes have an absolutely large proportion in alkanes.

3.1.3. Distribution of cycloalkanes

In contrast to the very small amount of branched alkanes, cycloalkanes were relatively abundant. When the temperature was below 485 °C, no cycloalkanes appeared in the oil components; when the temperature reached 485 °C, cycloalkanes were generated and their variety and total content grew with increasing temperature. At temperatures of 590, 650 and 764 °C, cycloalkanes occupied a relatively large proportion in the oil components. The distribution of cycloalkanes is shown in Table 2. It can be seen that with the increase of temperature, the content of most cycloalkanes increased, indicating that the cyclization reaction was accelerated at higher temperatures. A kind of bicyclic alkane, cis-bicyclo[10.8.0]eicosane, was detected in the oil components at 590 °C, 650 °C and 764 °C, and its proportion also increased with increasing temperature.

Cycloalkanes are partly produced by the separation of cycloalkyls from kerogen and partly generated by the cyclization reactions of alkanes and alkenes. At higher temperatures, plenty of alkyls depart from kerogen, and the amount of alkenes increases. This will provide more suitable conditions for the cyclization reactions.

Table 2. Distribution of cycloalkanes at different Curie-point temperatures

Compound	Content, area%			
	485 °C	590 °C	650 °C	764 °C
Cyclohexane, 1,4-bis(methylene)-		0.89	1.53	1.18
Cyclopropane, 1-methyl-2-pentyl-		2.19	1.13	
Cyclooctane, 1,2-dimethyl-	0.78	1.33	1.40	1.85
Cyclopropane, 1-heptyl-2-methyl-		1.45	1.63	2.44
Cyclododecane		1.39	1.52	1.90
Cyclotetradecane		0.17		
Cyclohexadecane		0.47		
Cyclopentadecane		0.62		
Bicyclo[10.8.0]eicosane, cis-		0.41	1.26	1.43
Cycloeicosane		1.35	1.51	1.90
Cyclotetracosane	0.92	0.62	2.10	1.42

3.2. Distribution of alkenes

Based on the experimental results, it was found that no alkenes were generated in the oil components when the Curie-point temperature was below 386 °C. But when the temperature was equal to or above 386 °C, alkenes appeared and both their variety and amount increased with the temperature rising. Figure 4 shows the distribution of alkenes at different Curie-point temperatures. Through comparison it could be discovered that at lower temperatures the alkenes with shorter carbon chains were quite few, but with increasing pyrolysis temperature, the amount of the relatively small molecule alkenes increased. Alkenes in shale oil were mainly generated in the cleavage of alkane molecules. The large molecule alkanes tend to be

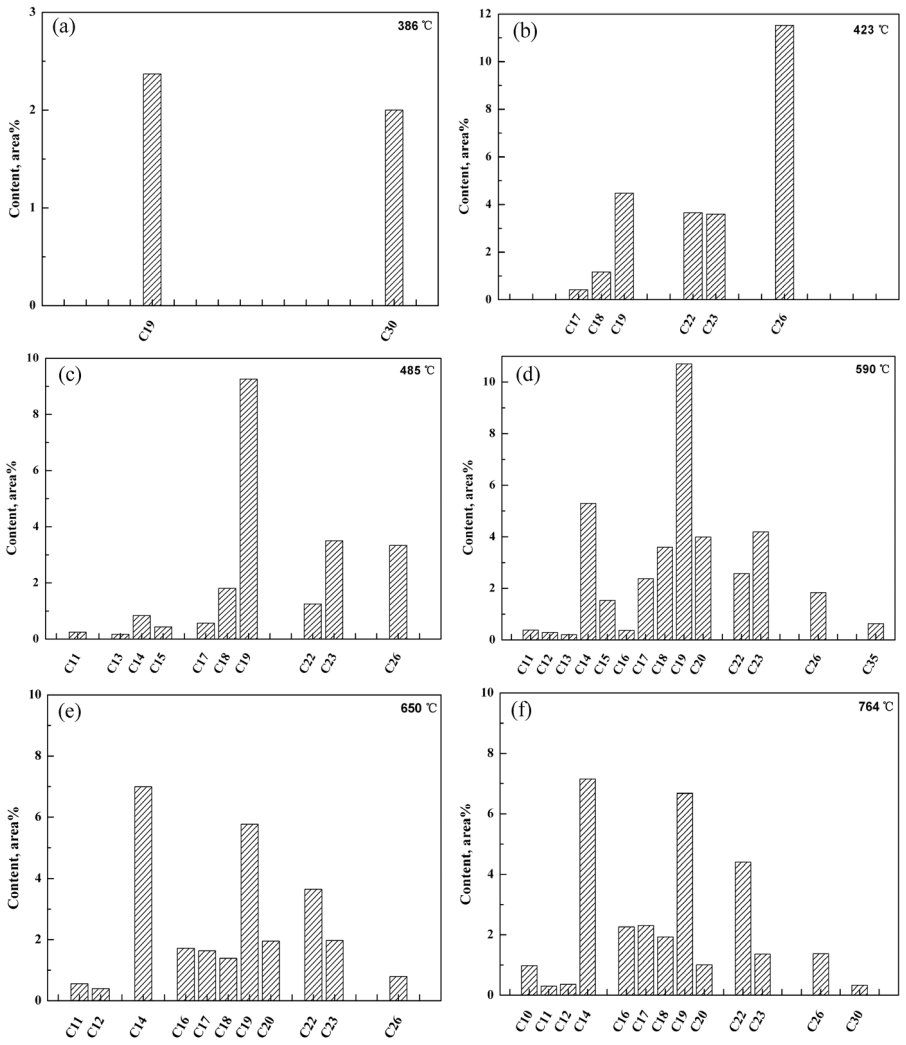

Fig. 4. Distribution of alkenes at different Curie-point temperatures.

decomposed, generating small molecule and unsaturated hydrocarbons. This is consistent with the conclusion presented below that α-alkenes formed the majority of all alkenes.

The proportion of alkenes in the oil components was high, the ratios being the following: 4.36% (386 °C), 24.85% (423 °C) 21.44% (485 °C), 33.46% (590 °C), 31.71% (650 °C) and 32.46% (764 °C). So it can be concluded that in the fast pyrolysis of oil shale, alkenes, which could be con verted to alkanes, occupy a large part in the oil to be utilized as liquid fuel after refining.

Among alkenes, mono-alkene constituted the largest proportion, while the ratio of alkadiene and polyene was quite small. The mono-alkene and alkadiene ratios at six different pyrolysis temperatures are listed in Table 3. There was only one kind of polyene, squalene, detected in the oil components at 386 °C, being also the only polyene found in the oil components under all conditions. It was clearly revealed that when the temperature reached 423 °C, the proportion of mono-alkene sharply increased and remained high at high temperatures. In mono-alkene components, α-alkenes occupied 100%, 74.3%, 72.1%, 52.1%, 51.2% and 54.2% of total mono-alkenes respectively at 386 °C, 423 °C, 485 °C, 590 °C, 650 °C and 764 °C. It can be concluded that α-alkenes mostly accounted for the majority of total mono-alkenes, and more intermediate olefins were generated at higher temperatures. This illustrated from another aspect that the scission reactions were easier to take place than the dehydrogenation reactions. Alkadienes appeared when the temperature reached 590 °C and then their amount grew fast with the increase of temperature. Alkadienes were mostly formed when the two C=C bonds appeared at the two ends of carbon chains. This was mainly because of the cleavage of α-alkenes in the high temperature pyrolysis.

Table 3. Mono-alkene and alkadiene proportions at different Curie-point temperatures

Temperature, °C	Mono-alkene, area%	Alkadiene, area%
386	2.37	–
423	24.85	–
485	21.44	–
590	31.47	1.51
650	27.90	3.81
764	25.96	6.50

3.3. Distribution of aromatic compounds

The identified aromatic compounds in the oils produced in the Curie-point pyrolysis experiments are listed in Table 4. It can be seen that aromatic compounds were generated when the temperature reached 423 °C and their varieties increased significantly with increasing temperature above 590 °C. Pyrolysis experiments with coal, kerogen and biomacromolecular substances

at about 600 to 700 °C are most common in the literature to study structural properties because it is thought that the product distribution could more closely reflect the various structural elements of macromolecular materials [35]. At both 423 °C and 485 °C only one kind of heterocyclic compound, 1,2-benzisothiazole, 3-(hexahydro-1H-azepin-1-yl)-, 1,1-dioxide, was identified, but when the temperature reached 590 °C, more than six aromatic compounds were detected. Hydrocarbyl benzene appeared in the oil compo-

Table 4. Distribution of aromatic compounds at different Curie-point temperatures

Temperature, °C	Compound	Content, area%
423	1,2-Benzisothiazole, 3-(hexahydro-1H-azepin-1-yl)-, 1,1-dioxide	1.59
485	1,2-Benzisothiazole, 3-(hexahydro-1H-azepin-1-yl)-, 1,1-dioxide	1.57
590	Indene	0.25
	Phenol, 4-methyl-	0.43
	Benzene, (1-methyl-2-cyclopropen-1-yl)-	0.50
	1-(4-Methoxy-phenyl)-6,6-dimethyl-2-(4-methyl-furazan-3-yl)-1,5,6,7-tetrahydro-indol-4-one	0.43
	Benzene, 1-butynyl-	0.19
	2,4-Dichlorobenzaldehyde 1-methyl-1-(2,4,6-trinitrophenyl)hydrazone	0.38
650	1H-Indene, 1,3-dimethyl-	0.27
	o-Xylene	1.08
	Indene	0.27
	Phenol, 2-methyl-	0.50
	Cycloprop[a]indene, 1,1a,6,6a-tetrahydro-	0.24
	Naphthalene, 1-methyl-	0.47
	Naphthalene, 2-methyl-	0.19
	Naphthalene, 2,6-dimethyl-	0.18
764	p-Xylene	3.70
	Benzene, 1-ethyl-4-methyl-	0.76
	Benzene, 1,1'-(1-ethenyl-1,3-propanediyl) bis-	1.43
	Indene	0.79
	Phenol, 2-methyl-	0.79
	Benzene, 1-butynyl-	1.90
	Naphthalene, 2-methyl-	0.59

nents at higher temperatures – 590 °C, 650 °C and 764 °C, and its amount also increased gradually with increasing temperature. Compared with the proportion of aliphatic compounds, the amount of aromatic compounds was quite small, which indicated that the aromaticity of the kerogen of Dachengzi oil shale was quite low. This conclusion is consistent with the ^{13}C NMR results of kerogen [30].

The high content of aliphatic hydrocarbons and low content of aromatic compounds reveal that the skeletal structure of oil shale kerogen is mainly composed of long-chain aliphatic alkyls and few aromatic rings. Through

analysis of the aromatic compounds generated at different Curie-point temperatures, especially at higher temperatures, it could be found that the condensed aromatic hydrocarbons of naphthalene existed in the macromolecular structure of kerogen. The substituent atoms of aromatic rings belonged mostly to aliphatic carbon and partly to organic oxygen. These results are in accord with the conclusions drawn by Tong et al. [30].

3.4. Distribution of oxygen-containing compounds

Compared with petroleum, shale oil contains a significantly higher amount of non-hydrocarbon constituents [36], of which oxygen-containing compounds represent a major portion. Oxygen-containing compounds, including ketones, acids, alcohols, esters and phenols, were found in the shale oils as the Curie-point pyrolysis products. The oxygen-containing compounds (phenols not included) identified in shale oil are listed in Table 5. It is clearly seen that these compounds began to be generated at the lowest temperature and made up a relatively big proportion in the products obtained at each temperature. The distribution of oxygen-containing compounds in Dachengzi shale oil was quite different from that in Mol and Bure oils obtained under different Curie-point pyrolysis conditions. The dominant oxygen-containing compounds in the pyrolysates of Mol and Bure kerogens were furanic derivatives, which were quite few in the Dachengzi oil shale pyrolysates. However, the ketones had the same existence form of n-alkan-2-one in the pyrolysates of all the three kerogens [27].

Table 5. Distribution of oxygen-containing compounds at different Curie-point temperatures

Temperature, °C	Compound	Molecular formula	Content, area%	Class
225	Hexadecanoic acid, methyl ester	$C_{17}H_{34}O_2$	20.36	Ester
	Ergosta-4,6,22-trien-3.beta.-ol	$C_{28}H_{44}O$	7.33	Alcohol
280	Methyl 11-eicosenoate	$C_{21}H_{40}O_2$	6.83	Ester
	Hexadecanoic acid, methyl ester	$C_{17}H_{34}O_2$	23.32	Ester
	Octadecanoic acid, methyl ester	$C_{19}H_{38}O_2$	3.18	Ester
	8-Octadecenoic acid, methyl ester, (E)-	$C_{19}H_{36}O_2$	7.01	Ester
315	2-Pentacosanone	$C_{25}H_{50}O$	5.02	Ketone
	2-Nonacosanone	$C_{29}H_{58}O$	3.85	Ketone
386	2-Pentacosanone	$C_{25}H_{50}O$	1.93	Ketone
	n-Hexadecanoic acid	$C_{16}H_{32}O_2$	2.79	Acid
	Eicosanoic acid	$C_{20}H_{40}O_2$	2.15	Acid
423	Triacontyl acetate	$C_{32}H_{64}O_2$	0.68	Ester
	Heptacosyl acetate	$C_{29}H_{58}O_2$	2.37	Ester
	Oleyl alcohol, heptafluorobutyrate	$C_{22}H_{35}F_7O_2$	2.44	Ester
	2-Nonacosanone	$C_{29}H_{58}O$	2.89	Ketone
	1-Hexacosanol	$C_{26}H_{54}O$	0.32	Alcohol
	1-Hexadecanol, 2-methyl-	$C_{17}H_{36}O$	0.85	Alcohol
485	Octacosyl acetate	$C_{30}H_{60}O_2$	0.96	Ester
	Oleyl alcohol, heptafluorobutyrate	$C_{22}H_{35}F_7O_2$	2.14	Ester

Table5. (Continuation)

Temperature, °C	Compound	Molecular formula	Content, area%	Class
	2-Nonacosanone	$C_{29}H_{58}O$	2.29	Ketone
	2-Pentacosanone	$C_{25}H_{50}O$	3.68	Ketone
	2-Nonadecanone	$C_{19}H_{38}O$	1.15	Ketone
	1-Dodecanol, 3,7,11-trimethyl-	$C_{15}H_{32}O$	1.20	Alcohol
590	Octacosyl acetate	$C_{30}H_{60}O_2$	0.50	Ester
	1-Heneicosyl formate	$C_{22}H_{44}O_2$	0.30	Ester
	cis-7-Dodecen-1-yl acetate	$C_{14}H_{26}O_2$	0.60	Ester
	Triacontyl acetate	$C_{32}H_{64}O_2$	0.44	Ester
	Methyl 5,13-docosadienoate	$C_{23}H_{42}O_2$	0.66	Ester
	2-Pentacosanone	$C_{25}H_{50}O$	0.79	Ketone
	2-Docosanone	$C_{22}H_{44}O$	0.20	Ketone
	2-Nonadecanone	$C_{19}H_{38}O$	0.55	Ketone
	Ergost-25-ene-3,5,6-triol, (3.beta.,5.alpha.,6.beta.)-	$C_{28}H_{48}O$	0.35	Alcohol
	Oleyl Alcohol	$C_{18}H_{36}O$	0.96	Alcohol
	E-2-Tetradecen-1-ol	$C_{14}H_{28}O$	0.55	Alcohol
	cis-9-Tetradecen-1-ol	$C_{14}H_{28}O$	0.72	Alcohol
	8-Dodecen-1-ol, (Z)-	$C_{12}H_{24}O$	0.39	Alcohol
650	Methyl (25RS)-3.beta.-hydroxy-5-cholesten-26-oate	$C_{28}H_{46}O_3$	0.32	Ester
	Octacosyl acetate	$C_{30}H_{60}O_2$	0.29	Ester
	Oleyl alcohol , acetate	$C_{20}H_{38}O_2$	0.65	Ester
	cis-7-Dodecen-1-yl acetate	$C_{14}H_{26}O_2$	0.88	Ester
	2-Pentacosanone	$C_{25}H_{50}O$	0.35	Ketone
	10-Undecen-1-ol	$C_{11}H_{22}O$	0.49	Alcohol
	Ergost-25-ene-3,5,6-triol, (3.beta.,5.alpha.,6.beta.)-	$C_{28}H_{48}O$	0.32	Alcohol
	n-Pentadecanol	$C_{15}H_{32}O$	1.81	Alcohol
	Oleyl Alcohol	$C_{18}H_{36}O$	0.68	Alcohol
764	E-7-Dodecen-1-ol acetate	$C_{14}H_{26}O_2$	1.17	Ester
	2-Pentacosanone	$C_{25}H_{50}O$	0.42	Ketone
	Eicosanoic acid	$C_{20}H_{40}O_2$	1.01	Acid
	n-Pentadecanol	$C_{15}H_{32}O$	2.25	Alcohol
	cis-9-Tetradecen-1-ol	$C_{14}H_{28}O$	0.80	Alcohol

Ester is one kind of the most important oxygen-containing compounds in oil components. Rose et al. [37] studied the bitumen samples extracted from the Queensland oil shale and the results revealed that the transmission spectra showed a strong absorption at about 1735cm^{-1} (due to the C=O stretch of esters), which is quite consistent with the results obtained in this article. CH_3COO-R esters were the major compounds of this kind existing in the oil components at the Curie-point temperatures equal to or above 423 °C. Ketones were abundant in the products obtained at temperatures higher than 315 °C. Through analysis of alcohols distribution, it was evident that there was a shift toward components with lower molecular weight as the temperature increased. In fact, oxygen-containing compounds are relatively thermo-sensitive, so that some of them are secondarily transformed at higher temperatures generating CO_2 [27]. The proportion of oxygen-containing

compounds in oil is determined by the maturity of oil shale, which means that in the oil components from higher maturity oil shale pyrolysis, these compounds are less abundant.

4. Conclusions

A series of CP-GC-MS experiments were conducted on the Dachengzi oil shale at the Curie-point temperatures of 225, 280, 315, 386, 423, 485, 590, 650 and 764 °C. It can be noticed that the pyrolysis reaction of oil shale is slow when the Curie temperature is below 386 °C, and becomes intense above 423 °C.

Aliphatic hydrocarbons dominate in the oil components at all the nine Curie temperatures, their amount increases significantly with increasing temperature. n-Alkanes are present in the oils at all the nine temperatures, while cycloalkanes and alkenes appear in the oils evolved above 485 °C and 386 °C, respectively. The proportions of cycloalkanes and alkenes increase with the pyrolysis temperature, corresponding to the decrease of n-alkanes at higher temperatures as a result of the cleavage reaction of alkanes. Branched alkanes seldom exist in the oils owing to the cleavage of the C–C bond at the branched point.

Aromatic compounds are generated in high amounts when the temperature is above 485 °C. The molecule size of aromatic compounds decreases with the increase of temperature so that compounds with a carbon number bigger than 10 were found in the products above 590 °C. Most of the aromatic compounds formed in the oil components under fast pyrolysis conditions belong to alkyl-benzenes, and few are alkyl-naphthalenes.

The abundant existence of oxygen-containing compounds, including ketones, acids, alcohols, esters and phenols, reveals that oxygen-containing functional groups abound in kerogen. Generally, –COO– and –C=O are the two kinds of most abundant oxygen-containing functional groups in the kerogen of Dachengzi oil shale.

Acknowledgements

This work was supported by the Shanghai Natural Science Foundation (Grant No. 13ZR1420300).

REFERENCES

1. Tiwari, P., Deo, M. Compositional and kinetic analysis of oil shale pyrolysis using TGA–MS. *Fuel*, 2012, **94**, 333–341.

2. Batts, B. D., Fathoni, A. Z. A literature review on fuel stability studies with particular emphasis on diesel oil. *Energ. Fuel.*, 1991, **5**(1), 2–21.
3. Dyni, J. R. Geology and resources of some world oil-shale deposits. *Oil Shale*, 2003, **20**(3), 193–252.
4. Altun, N. E., Hicyilmaz, C., Hwang, J.-Y., Bagci, A. S., Kök, M. V. Oil shales in the world and Turkey; reserves, current situation and future prospects: a review. *Oil Shale*, 2006, **23**(3), 211–227.
5. Yu, H., Li, S. Y., Jin, G. Z. Catalytic hydrotreating of the diesel distillate from Fushun shale oil for the production of clean fuel. *Energ. Fuel.*, 2010, **24**(8), 4419–4424.
6. Chen, X. B., Shen, B. X., Sun, J. P., Wang, C. X., Shan, H. H., Yang, C. H., Li, C. Y. Characterization and comparison of nitrogen compounds in hydrotreated and untreated shale oil by electrospray ionization (ESI) Fourier transform ion cyclotron resonance mass spectrometry (FT-ICR MS). *Energ. Fuel.*, 2012, **26**(3), 1707–1714.
7. Rovere, C. E., Crisp, P. T., Ellis, J., Korth, J. Chemical class separation of shale oils by low pressure liquid chromatography on thermally-modified adsorbants. *Fuel*, 1990, **69**(9), 1099–1104.
8. Fletcher, T. H., Gillis, R., Adams, J., Hall, T., Mayne, C. L., Solum, M. S., Pugmire, R. J. Characterization of macromolecular structure elements from a Green River oil shale, II. Characterization of pyrolysis products by ^{13}C NMR, GC/MS, and FTIR. *Energ. Fuel.*, 2014, **28**(5), 2959–2970.
9. Tong, J. H., Liu, J. G., Han, X. X., Wang, S., Jiang, X. M. Characterization of nitrogen-containing species in Huadian shale oil by electrospray ionization Fourier transform ion cyclotron resonance mass spectrometry. *Fuel*, 2013, **104,** 365–371.
10. Lédé, J., Broust, F., Ndiaye, F.-T., Ferrer, M. Properties of bio-oils produced by biomass fast pyrolysis in a cyclone reactor. *Fuel*, 2007, **86**(12–13), 1800–1810.
11. Li, M. W., Cheng, D. S., Pan, X. H., Dou, L. R., Hou, D. J., Shi, Q., Wen, Z. G., Tang, Y. J., Achal, S., Milovic, M., Tremblay, L. Characterization of petroleum acids using combined FT-IR, FT-ICR–MS and GC–MS: Implications for the origin of high acidity oils in the Muglad Basin, Sudan. *Org. Geochem.*, 2010, **41**(9), 959–965.
12. Butler, E., Devlin, G., Meier, D., McDonnell, K**.** Fluidised bed pyrolysis of lignocellulosic biomasses and comparison of bio-oil and micropyrolyser pyrolysate by GC/MS-FID. *J. Anal. Appl. Pyrol.*, 2013, **103**, 96–101.
13. Geng, C. C., Li, S. Y., Ma, Y., Yue, C. T., He, J. L., Shang, W. Z. Analysis and identification of oxygen compounds in Longkou shale oil and Shenmu coal tar. *Oil Shale*, 2012, **29**(4), 322–333.
14. Zheng, D. W., Li, S. Y., Ma, G. L., Wang, H. Y. Autoclave pyrolysis experiments of Chinese Liushuhe oil shale to simulate in-situ underground thermal conversion. *Oil Shale*, 2012, **29**(2), 103–114.
15. Williams, P. T., Nazzal, J. M. Polycyclic aromatic compounds in oils derived from the fluidised bed pyrolysis of oil shale. *J. Anal. Appl. Pyrol.*, 1995, **35**(2), 181–197.
16. De la Rosa, J. M., Knicker, H., López-Capel, E., Manning, D. A. C., González-Perez, J. A., González-Vila, F. J. Direct detection of black carbon in soils by Py-GC/MS, carbon-13 NMR spectroscopy and thermogravimetric techniques. *Soil Sci. Soc. Am. J.*, 2008, **72**(1), 258–267.

17. Lu, Q., Li, W. Z., Zhang, D., Zhu, X. F. Analytical pyrolysis–gas chromatography/mass spectrometry (Py–GC/MS) of sawdust with Al/SBA-15 catalysts. *J. Anal. Appl. Pyrol.*, 2009, **84**(2), 131–138.
18. Wang, S. R., Guo, X. J., Liang, T., Zhou, Y., Luo, Z. Y. Mechanism research on cellulose pyrolysis by Py-GC/MS and subsequent density functional theory studies. *Bioresource Technol.*, 2012, **104**, 722–728.
19. Ross, A. B., Anastasakis, K., Kubacki, M., Jones, J. M. Investigation of the pyrolysis behaviour of brown algae before and after pre-treatment using PY-GC/MS and TGA. *J. Anal. Appl. Pyrol.*, 2009, **85**(1–2), 3–10.
20. Strezov, V., Lucas, J. A., Evans, T. J., Strezov, L. Effect of heating rate on the thermal properties and devolatilisation of coal. *J. Therm. Anal. Calorim.*, 2004, **78**(2), 385–397.
21. Yu, J. *Study and Modelling on the Interaction of Volatile Flame, CO Flame and Char Particle Combustion*, PhD dissertation. Shanghai JiaoTong University, 2003.
22. Niksa, S., Lau, C.-W. Global rates of devolatilization for various coal types. *Combust. Flame*, 1993, **94**(3), 293–307.
23. Yanik, J., Yüksel, M., Sağlam, M., Olukçu, N., Bartle, K., Frere, B. Characterization of the oil fractions of shale oil obtained by pyrolysis and supercritical water extraction. *Fuel*, 1995, **74**(1), 46–50.
24. Wang, H., Jiang, X. M., Liu, H., Wu, S. H. Fast pyrolysis comparison of coal–water slurry with its parent coal in Curie-point pyrolyser. *Energ. Convers. Manage.*, 2009, **50**(8), 1976–1980.
25. Xu, W. C., Tomita, A. Effect of temperature on the flash pyrolysis of various coals. *Fuel*, 1987, **66**(5), 632–636.
26. Hempfling, R., Schulten, H.-R. Chemical characterization of the organic matter in forest soils by Curie point pyrolysis-GC/MS and pyrolysis-field ionization mass spectrometry. *Org. Geochem.*, 1990, **15**(2), 131–145.
27. Deniau, I., Devol-Brown, I., Derenne, S., Behar, F., Largeau, C. Comparison of the bulk geochemical features and thermal reactivity of kerogens from Mol (Boom Clay), Bure (Callovo–Oxfordian argillite) and Tournemire (Toarcian shales) underground research laboratories. *Sci. Total Environ.*, 2008, **389**(2–3), 475–485.
28. Pouwels, A. D., Eijkel, G. B., Boon, J. J. Curie-point pyrolysis-capillary gas chromatography-high-resolution mass spectrometry of microcrystalline cellulose. *J. Anal. Appl. Pyrol.*, 1989, **14**(4), 237–280.
29. Liu, J. L., Jiang, J. C., Huang, H. T. Selective pyrolysis behaviors of willow catalyzed via phosphoric acid. *Adv. Mat. Res.*, 2013, **724–725**, 413–418.
30. Tong, J. H., Han, X. X., Wang, S., Jiang, X. M. Evaluation of structural characteristics of Huadian oil shale kerogen using direct techniques (solid-state ^{13}C NMR, XPS, FT-IR, and XRD). *Energ. Fuel.*, 2011, **25**(9), 4006–4013.
31. Cady, W. E., Seelig, H. S. Composition of shale oil. *Ind. Eng. Chem.*, 1952, **44**(11), 2636–2641.
32. Yürüm, Y., Levy, M. Analysis of a retort oil from an Israeli shale by gas chromatography-mass spectrometry-selected ion monitoring. *Fuel*, 1985, **64**(1), 102–107.
33. Rebick, C. Pyrolysis of heavy hydrocarbons. In: *Pyrolysis: Theory and Industrial Practice* (Albright, L. F., Crynes, B. L., Corcoran, W. H., eds.). Academic Press, 1983, 69–87.

34. Fookes, C. J. R., Duffy, G. J., Udaja, P., Chensee, M. D. Mechanisms of thermal alteration of shale oils. *Fuel*, 1990, **69**(9), 1142–1144.
35. Hatcher, P. G., Clifford, D. J. Flash pyrolysis and *in situ* methylation of humic acids from soil. *Org. Geochem.*, 1994, **21**(10–11), 1081–1092.
36. Van Meter, R. A., Bailey, C. W., Smith, J. R., Moore, R. T., Allbright, C. S., Jacobson, I. A., Hylton, V. M., Ball, J. S. Oxygen and nitrogen compounds in shale-oil naphtha. *Anal. Chem.*, 1952, **24**(11), 1758–1763.
37. Rose, H. R., Smith, D. R., Vassallo, A. M. An investigation of thermal transformations of the products of oil shale demineralization using infrared emission spectroscopy. *Energ. Fuel.*, 1993, **7**(2), 319–325.

Presented by Y. O. Solantausta
Received May 12, 2014